J Mol Model (2009) 15:1447–1462
DOI 10.1007/s00894-009-0500-7

ORIGINAL PAPER

An ab initio quantum mechanical drug designing procedure: application to the design of balanced dual ACE/NEP inhibitors

Nishi K. Rao · Arpita Yadav · Sanjeev Kumar Singh

Received: 5 July 2008 / Accepted: 3 March 2009 / Published online: 9 May 2009

Abstract This article describes in a sequential fashion how ab initio quantum mechanical methods can be applied to study the pharmacophoric features of drugs. It also describes how accurate drug–receptor interaction calculations can guide the careful design of balanced dual inhibitors, which form an important class of second generation drugs. As an example, the authors have chosen balanced inhibitors of angiotensin converting enzyme/neutral endopeptidase (ACE/NEP) as modern antihypertensive drugs. A unified, accurate, in silico design approach is presented, encompassing all steps from pharmacophore derivation to complete understanding of mechanistic aspects leading to drug design.

Keywords Ab initio · Drug–receptor interaction · ACE/NEP dual inhibitor · ACE receptor model · Modern antihypertensive

Electronic supplementary material The online version of this article (doi:10.1007/s00894-009-0500-7) contains supplementary material, which is available to authorized users.

N. K. Rao · A. Yadav (✉)
Department of Chemistry,
University Institute of Engineering and Technology,
CSJM University,
Kanpur 208024, India
e-mail: arpitayadav@yahoo.co.in

S. Kumar Singh
Centre of Excellence in Bioinformatics,
Department of Genetic Engineering,
School of Biotechnology, Madurai Kamaraj University,
Tamil Nadu,
Madurai 625 021, India

Introduction

The process of designing new drugs is often hampered by long rounds of drug synthesis and testing, with subsequent modifications followed by further rounds of synthesis and activity evaluation [1]. This seemingly endless cycle of refining continues until the desired level of drug potency is achieved [2, 3]. Such molecular pharmacology procedures are often coupled with quantitative structure–activity relationships (QSARs) based on experimentally determined parameters that are closely related to drug potency [4]. QSARs are mathematical models that use chemical structures or molecular properties as descriptors to define the relationship to biological activity. Crippen [5] has shown recently how chirality can be defined quantitatively and used as a descriptor. For appropriate application of QSARs to drug design, quantitative sequence–activity models (QSAMs) [6] of biosystems have been explored but have turned out to be extremely complex. It was soon realised that pharmacokinetic descriptors would be needed in order to make such studies useful. Automated virtual screening of libraries of compounds based on important structural features indicated by QSAR studies can also be carried out to assist synthetic studies in the choice of lead compounds [7].

Several automated docking algorithms [8, 9] are available and are used frequently in drug designing studies. However, the scoring functions used in these studies remain questionable depending on the parameters used to define protein–ligand binding affinity.

Molecular dynamics simulations coupled with homology modelling studies have been carried out in a number of cases to understand the mechanistic details of drug–target

interactions [10]. However, in cases where the target protein shares only low similarity with the template sequence, many problems have been encountered [11].

The above gives some examples of the methodologies and techniques applied to drug design studies. In this article, we present and discuss the application of ab initio quantum mechanical molecular orbital techniques and ab initio intermolecular interaction calculations to drug–receptor interactions for drug design. The procedure, part of which was published earlier along with different applications [12, 13], was designed with the aim of determining accurate drug–receptor interaction calculations from the perspective that the latter are the key to a drug's mechanism and potency. In this study, we have summarised the entire procedure from application of the ab initio quantum mechanical procedure to designing dual angiotensin converting enzyme/neutral endopeptidase (ACE/NEP) inhibitors. Inhibition of these two enzymes is synergistic in nature, and balanced dual inhibitors, as opposed to specific inhibition of one or the other, are proving valuable as second generation antihypertensive drugs [14].

ACE/NEP inhibition

Angiotensin converting enzyme plays a pivotol role in regulating blood pressure [15]. ACE—a zinc metalloprotease belonging to the gluzincin family where catalysis is mediated by HEXXH motif—catalyses proteolysis of angiotensin I (ANG I) to form the vasoconstrictor angiotensin II (ANG II), hence playing a major role in the renin–angiotensin system (RAS). ACE inhibitors are used quite widely in the clinical treatment of cardiovascular diseases and in blood pressure control [16, 17] but their use is commonly associated with side effects like angioedema and dry cough [18]. These side effects have been associated with abnormal degradation of bradykinin active metabolite in hypertensive patients treated with ACE inhibitors [19]. This response is induced biologically due to the reduced activity of ACE. Neutral endopeptidase (NEP) inhibition potentiates atrial natriuretic peptide (ANP) and bradykinin, leading to synergistic effects concomitant with ACE inhibition [20]. Therefore, second generation antihypertensives should constitute balanced dual ACE/NEP inhibitors, i.e. blocking ANG II production while at the same time potentiating endogenous ANP levels. Balanced dual inhibition means moderate activity at both receptors as opposed to little activity at one receptor and a lot at the other. Balanced dual inhibitors reduce the chances of side effects.

This study describes the application of modern ab initio quantum mechanical techniques to designing balanced dual inhibitors by accurately calculating drug–receptor interactions and correlating these mechanistically to potency.

Methods

The entire procedure is shown in the form of a flow chart in Fig. 1. Several clinically used drugs and drugs undergoing in vitro analysis covering a whole range of potency were chosen, some of which target ACE while others target NEP (Fig. 2). All experimental potency data has been taken from refs [21–35]. We have to understand the mode of action of each individual inhibitor in order to be able to design balanced dual inhibitors.

The stepwise methodology is described in the following sections:

Choice of compounds and determination of bioactive conformation

The set of compounds chosen for this study were compounds that are preferably in clinical use, chemically diverse and covering a wide potency range. The goal was to search for common, essential pharmacophoric features. Complete geometry optimisations [36, 37] were performed for the probable bioactive conformation of each drug at the Hartree Fock (HF) level utilising the 6–31G* basis set [38, 39]. Some calculations were also carried out utilising the non-local hybrid HF density functional theory (DFT) functional (B3LYP level) [40]. The bioactive conformation of a drug can be judged by visual examination of models of several drugs bound to an enzyme. In cases where visual examination revealed the suitability of more than one compound in terms of binding to enzyme active site, we optimised and docked more than one conformation of the drug. Some conformations can be eliminated easily by visual examination of natural constraints imposed due to the receptor/enzyme active site. In the present study, the zinc binding group must also be facing a metal ion otherwise the drug cannot bind. Active site space limitations play a major role in the choice of bioactive conformation. If elimination of a particular conformation is obvious after viewing the active site then docking is not necessary. However, researchers in this area should feel free to try out other possibilities that remain in their opinion.

Conformational mapping and pharmacophore model derivation

All optimised conformations are overlapped on the most potent or prototype drug to get an idea of the variations in conformation. This is referred to as conformational mapping. If X-ray coordinates of any drug bound to the receptor are available then the bioactive conformation is known and the optimised conformation can be compared accordingly. The charge environment of the drug is studied by

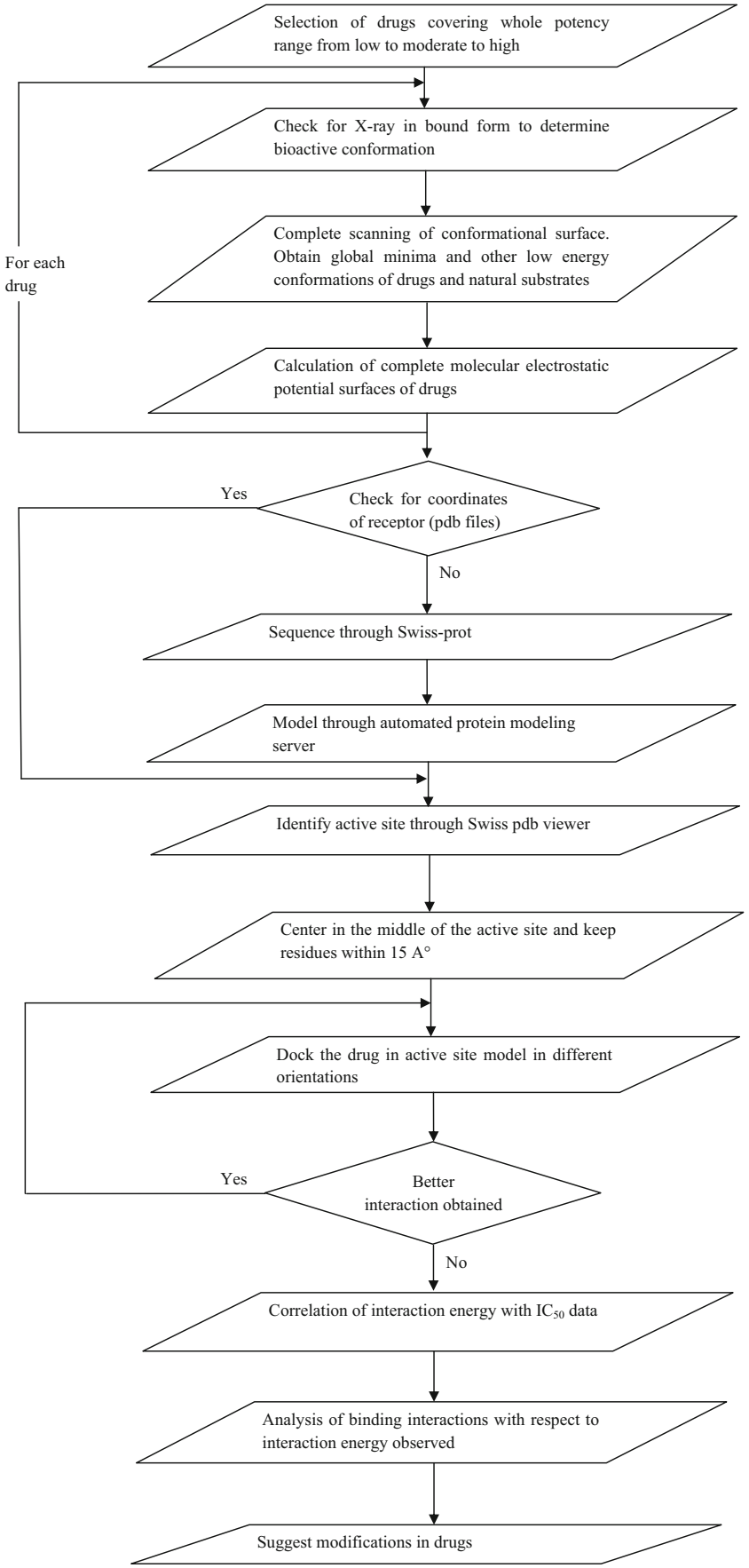

Fig. 1 An ab initio quantum mechanical procedure for drug design

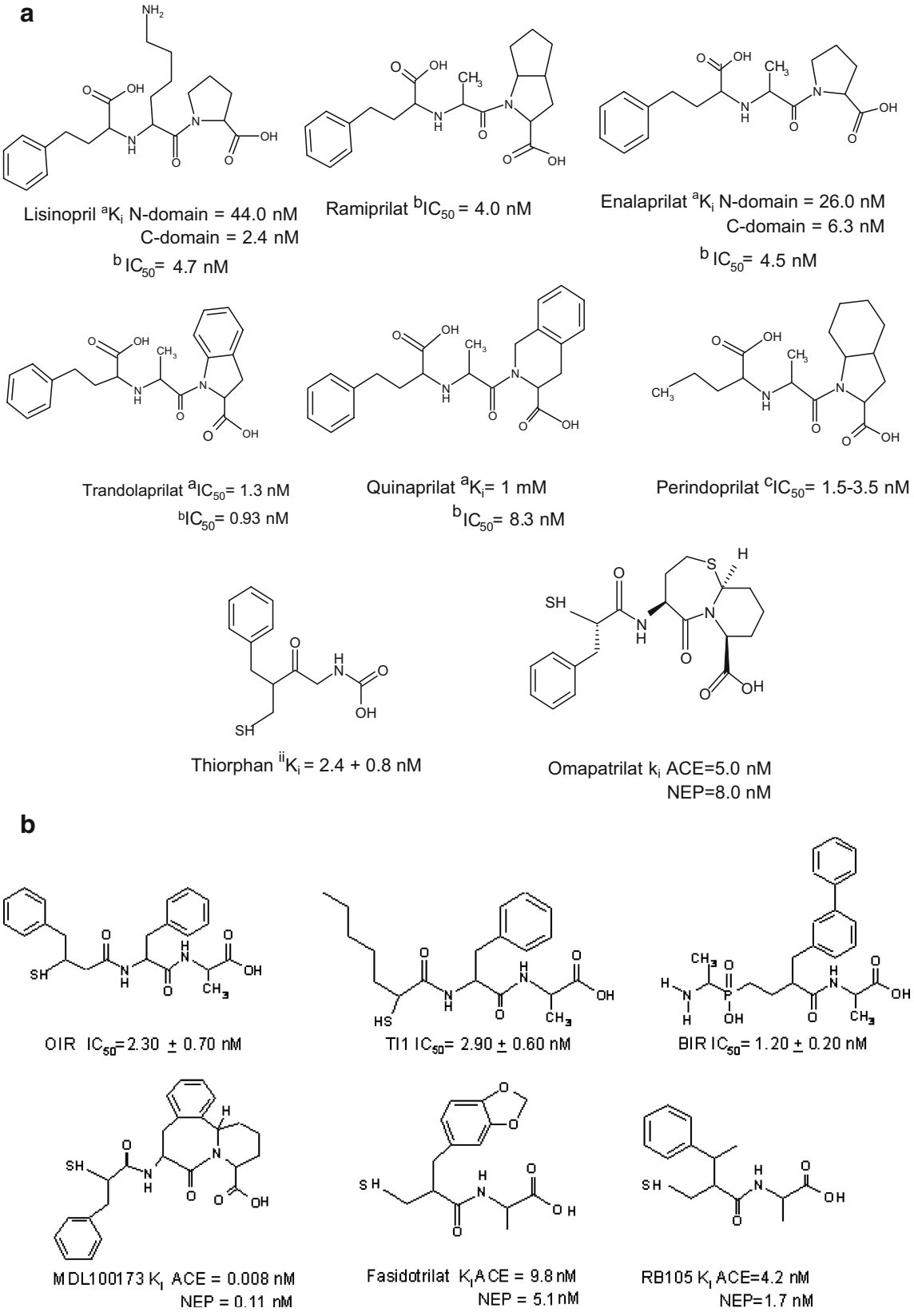

Fig. 2 Clinically used angiotensin converting enzyme (ACE)-, neutral endopeptidase (NEP)- and dual-inhibitors

calculating molecular electrostatic potential derived charges [41]. Based on the conformational mapping and charge distribution of the drug, common and essential pharmacophoric features are deduced and can be presented in the form of a pharmacophore model. Non skeletal schematic pharmacophore models have been derived that indicate only the location and number of essential functional groups and overall dimensions. The exact disposition of functional groups can be elucidated through skeletal models only if a common chemical skeleton is observed. Automated pharmacophore model generation has also been done by utilising the PHASE module of Schrodinger [42, 43] software for the sake of comparison.

Extracting the active site and preparing a receptor model

To understand the mechanism of action, and to elucidate the importance of pharmacophoric features derived above, models of enzyme active sites based on available X-ray data were made so that docking studies could be performed. Available X-ray coordinates are located in the protein data bank (pdb) and the corresponding pdb files were downloaded and viewed using Swiss pdb viewer [44] to identify the active site catalytic motif (HEXXH motif in this case). The model covers approximately 12–15 Å around the active site motif, maintaining the complex 3D environment around the latter. This all-atom, active site model is treated ab initio to maintain the physiological conditions under which the drug acts. The residues that are ionised are maintained in their charged form by ensuring proper bonding and number of hydrogens when modifying the extracted pdb file for ab initio calculations. Overall charges on receptor and drug and a closed shell system are specified when doing molecular orbital calculations. Water molecules embedded in the protein within this range are also retained, as they may occasionally be mechanistically important by mediating H-bonds. Hydrogens

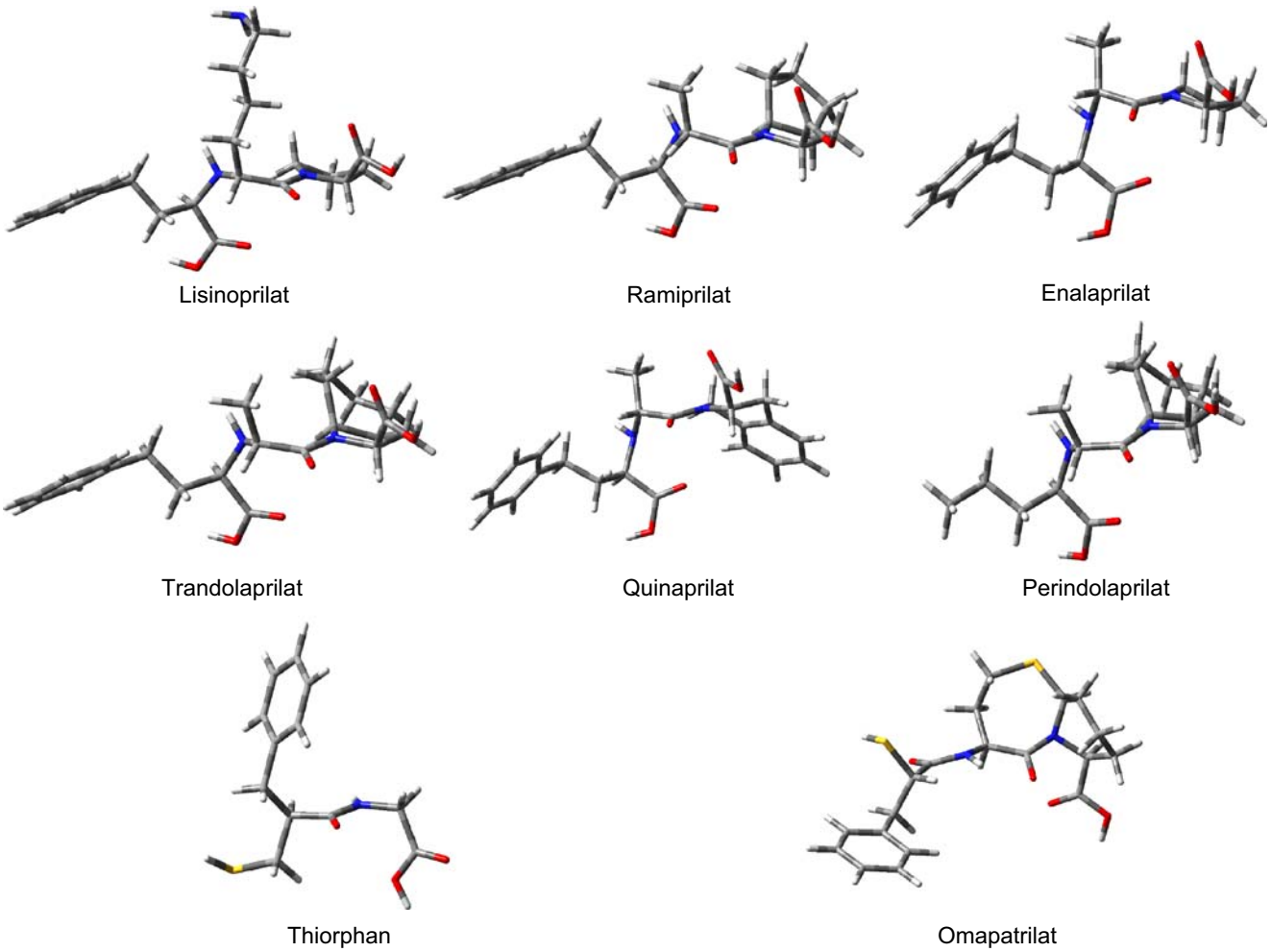

Fig. 3 Optimised bioactive conformations of ACE-, NEP- and dual-inhibitors

are added using GAUSSVIEW [45], and bonding is rectified at sites of poor X-ray resolution.

Docking and drug–receptor interaction energy calculations

Selected drugs were docked in the model one by one in different orientations until the best interaction with the catalytic site was obtained. The criterion for docking was that the drug should not be linked covalently, and must show an attractive interaction with catalytic residues and the metal ion that is known to mediate catalysis in this case. Drug–receptor interaction energy was calculated using a supermolecule approach at the HF level

$$E_{\text{int en.}} = E_{\text{complex}} - \left(E_{\text{drug}} + E_{\text{receptormodel}}\right)$$

All calculations were performed using GAUSSIAN '03 [46] software.

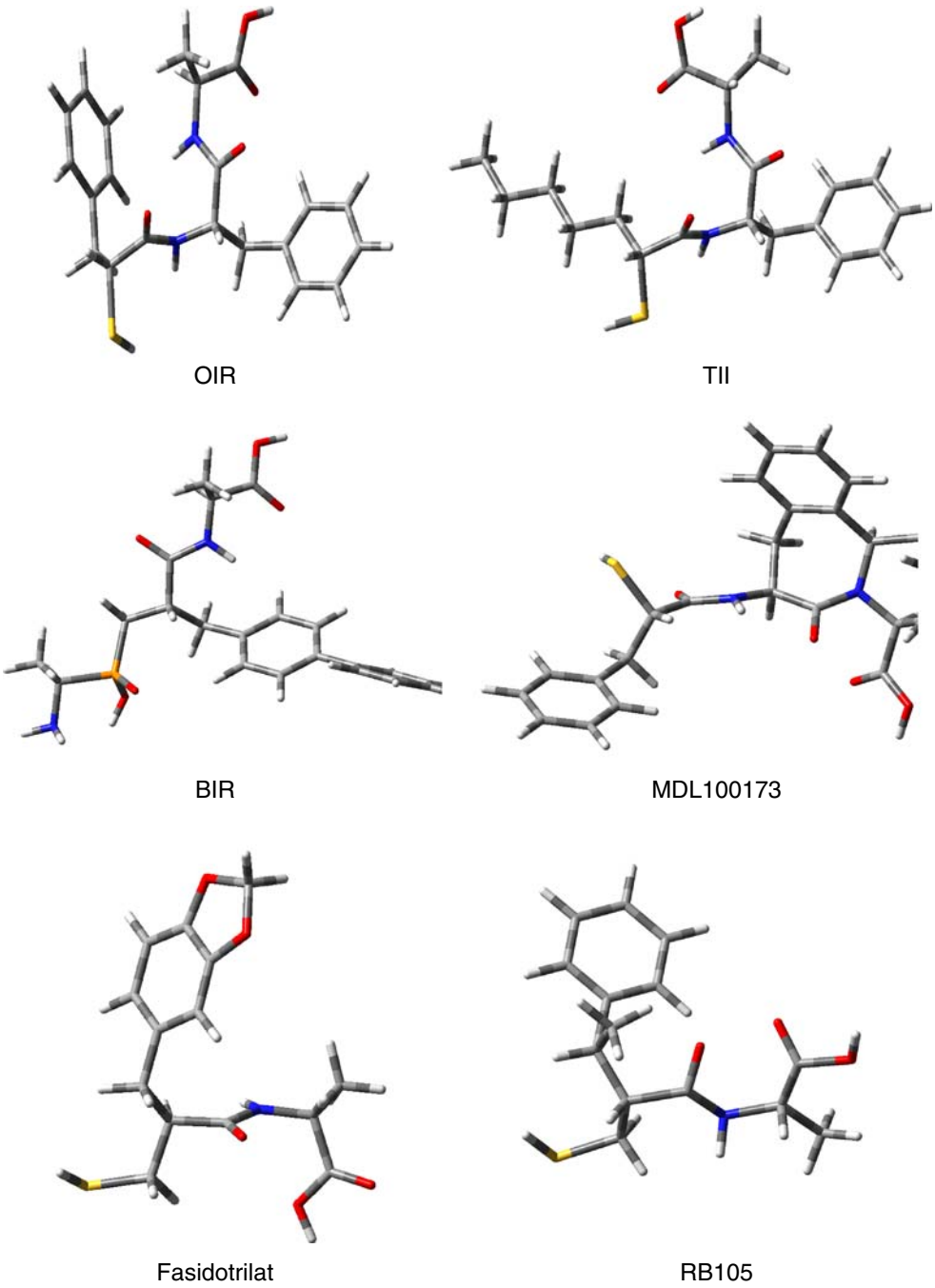

Fig. 4 Optimised bioactive conformations of ACE-, NEP- and dual-inhibitors undergoing in vitro analysis

Drug/scaffold design and in silico testing

Based on the above findings, modifications in existing drugs may be implemented or new scaffolds or drugs may be designed. Designed drugs were also completely optimised, mapped and docked. The potential efficacy of the designed drug was tested by repeated docking and evaluation of drug–receptor interactions.

Correlating calculated drug–receptor interaction energies with experimental potency data

Finally, calculated drug–receptor interaction energies were correlated with IC_{50} values to evaluate the performance of the model. This comparison accurately illustrates the importance of interaction energy calculations at the microscopic level. However, when using potency data, care must be exercised to keep track of the experimental error bars of various measurements. It is best to compare data from the same source.

Results and discussion

This paper presents an attempt towards designing balanced dual ACE/NEP inhibitors. The optimized bioactive conformations of clinically used drugs are shown in Fig. 3. The starting point for optimisation of these ACE inhibitors was judged based on several available X-ray structures [Lisinopril in testicular (t)-ACE 2C6N.pdb; Enalaprilat in t-ACE

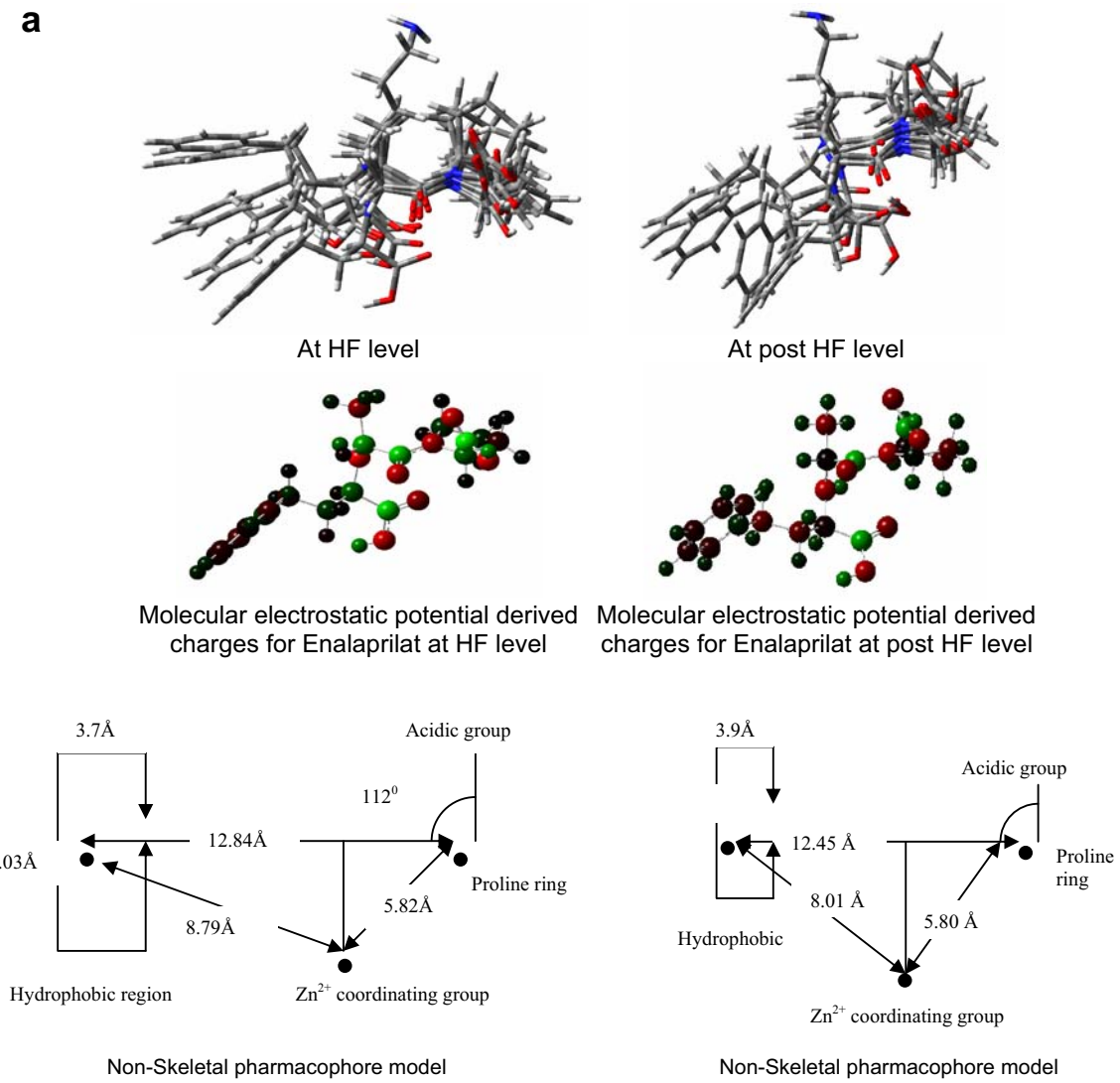

Fig. 5 **a** Pharmacophore model derivation for C-domain specific ACE inhibitors at 6–31G and B3LYP levels. **b** Automated pharmacophore model derivation for ACE inhibitors. **c** Protein based pharmacophore of 1UZE with Enalaprilat (as bound ligand). *Red arrows* Hydrogen bond acceptors, *green arrows* hydrogen bond donors, *yellow spheres* hydrophobic features, *blue regions* positive ionisable areas, *red regions* negative ionisable regions, *light blue cone* metal binding feature

Fig. 5 (continued)

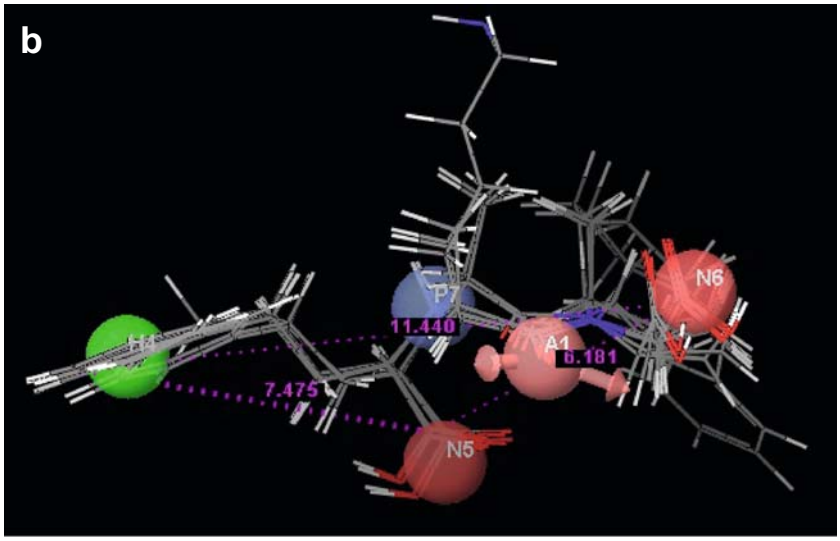

Model I (AHNNP)

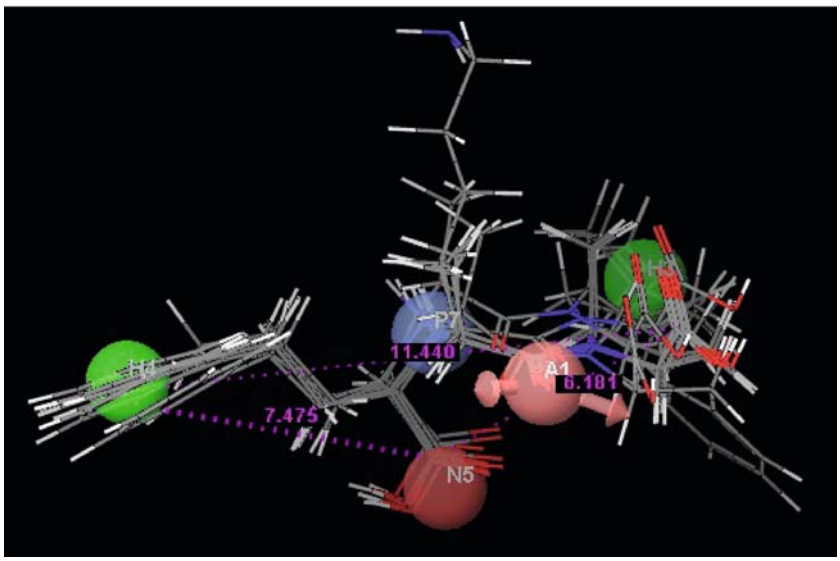

Model II (AHHNP)

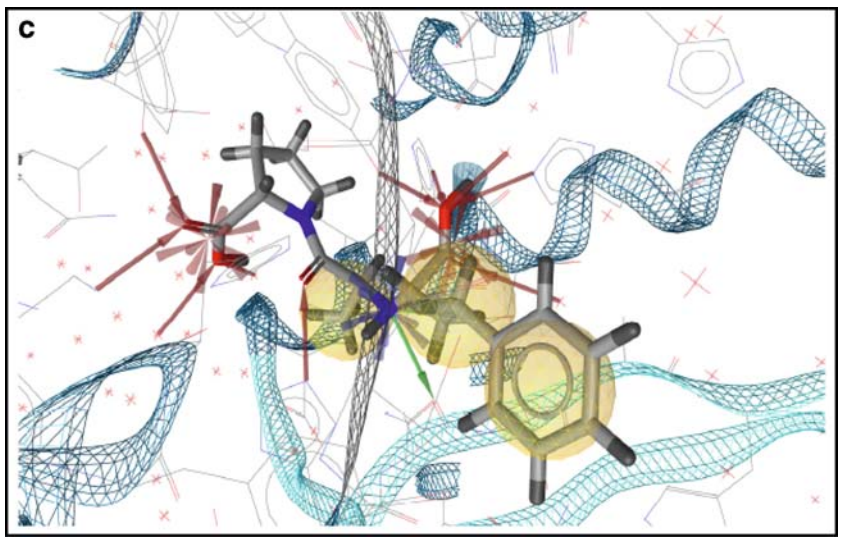

1UZE.pdb; Captopril in ACE 1UZF.pdb; TI1 in NEP 1R1I.pdb; OIR in NEP 1R1J.pdb; BIR in NEP 1R1H.pdb]. Optimized 'probable' bioactive conformations of drugs undergoing in vitro analysis are shown in Fig. 4. Non skeletal pharmacophore model derivation based on conformational mapping and charge environment for ACE inhibitors at HF and B3LYP levels is shown in Fig. 5. Although isolated drug calculations can be performed at higher levels, we restricted ourselves to this level so that the entire study, including calculations on ANG I could be performed at this level. Mapping helps identify common essential features. It also guides our understanding of the dimensions of hydrophobic regions. Analysis of the charge environment helps identify metal coordinating group and recognises other complementarity criteria. Similarly, pharmacophore model derivations for NEP and dual inhibitors are shown in Fig. 6.

For ACE inhibitors, we also performed an automated pharmacophore model derivation using the PHASE 3.0 module of the program SCHRÖDINGER. Two models were generated, with almost equal survival scores: model I (AHNNP) contains one hydrogen bond acceptor (A), one hydrophobic group (H), two negative sites (NN) and one positive site (P), while model II (AHHNP) contains one hydrogen bond acceptor (A), two hydrophobic groups (HH), one negative site (N) and one positive site (P). Ramipril, an example of a potent drug in clinical use, showed the best fitness score compared to other compounds. The derived pharmacophore models are shown in Fig. 5b. All distances and angles between pharmacophoric sites are given in suppl. 4 of the electronic supplementary material (ESM). The automated pharmacophore highlights the same features overall as the manually derived pharmacophore model. The metal binding group is again identified as the major negative site. The derived pharmacophore was also illustrated inside the active site in Fig. 5c, showing the metal binding region.

Before comparing pharmacophoric features, the following points should be noted:

Figure 5 depicts no significant change in pharmacophoric features at the B3LYP level as compared to HF 6–31G* calculations. Drastic changes in pharmacophoric features are not expected at higher levels. Secondly, the main aim of this procedure is to construct a good model of the enzyme that

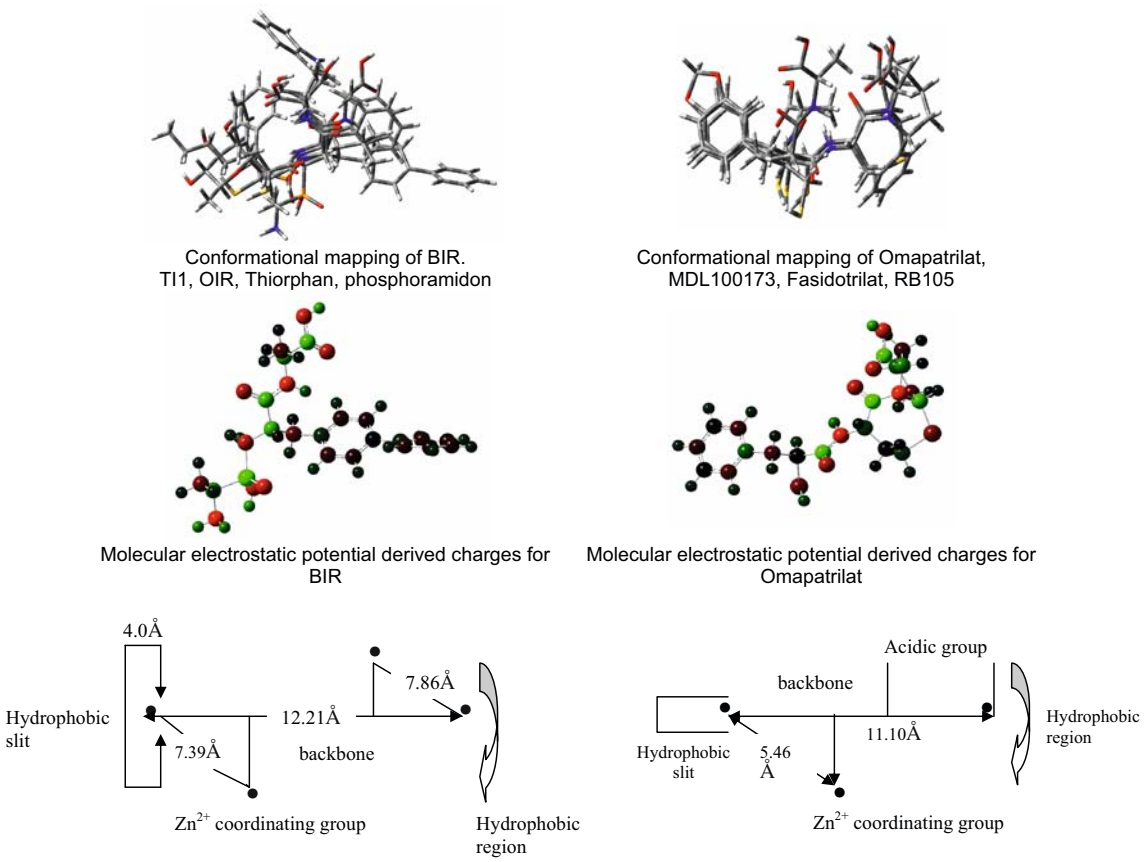

Fig. 6 Non skeletal pharmacophore model derivation for NEP- and dual-inhibitors

preserves the active site environment up to ~15 Å and in which all atoms can be treated ab initio after docking in the peptidomimetic drug. These calculations have to be repeated several times for each drug as the drug is docked in different orientations. Therefore, to maintain a balance between computational cost and effectiveness, all further calculations were performed at the HF 6–31G level [47, 48].

We next performed a comparative analysis of the pharmacophoric features of ACE-, NEP- and dual-inhibitors. Most ACE inhibitors are β-turn mimetics, with

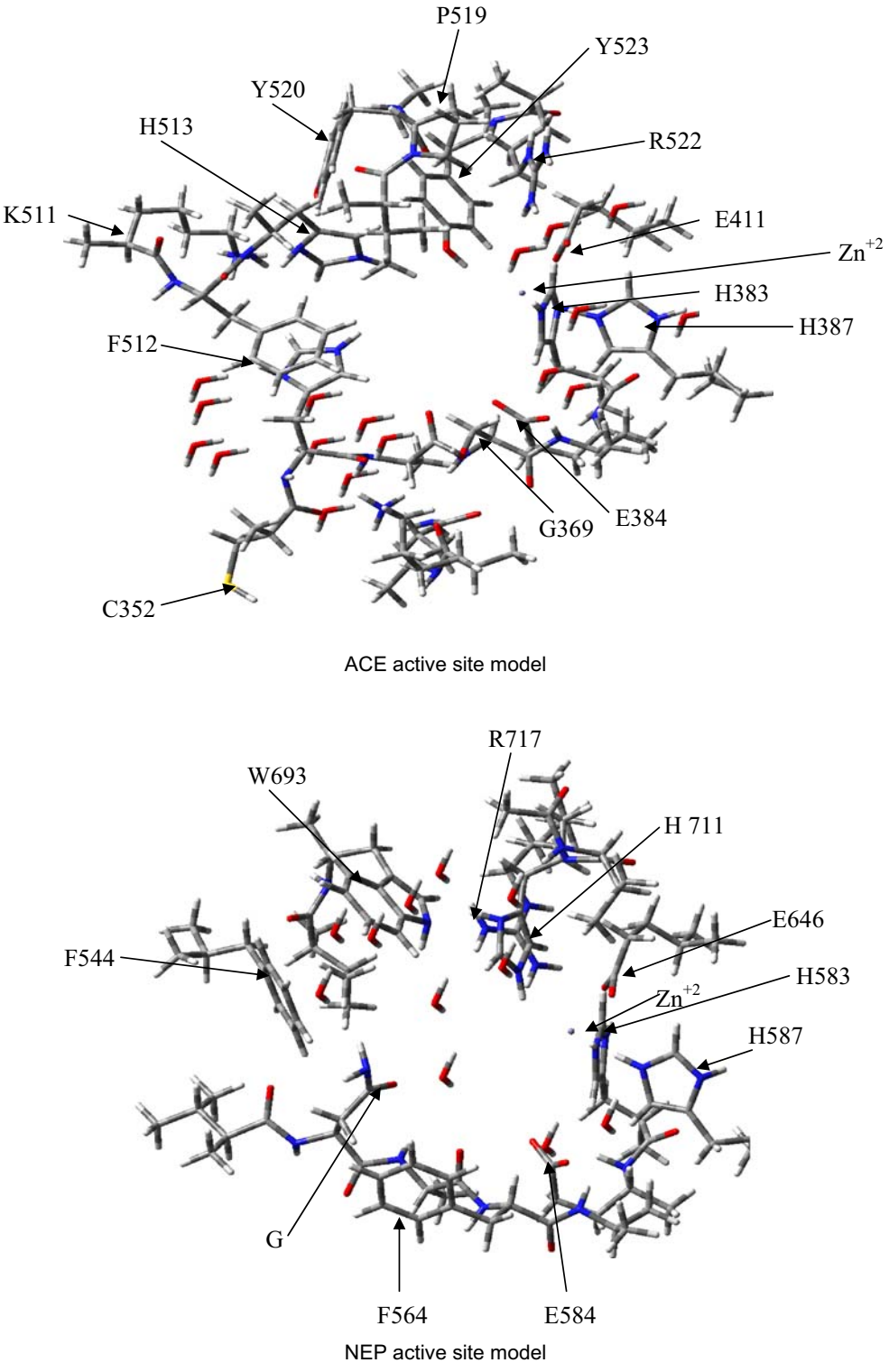

Fig. 7 ACE and NEP receptor models prepared from quantum mechanical calculations

a proline-type ring at one end and a hydrophobic group at the other end separated by ~12.8 Å. The different orientations of the hydrophobic group indicate that the hydrophobic region in the enzyme active site must be quite large so as to be able to accommodate each of these orientations. Another important pharmacophoric feature is the metal ion coordinating group present at ~6 Å from the proline ring. The relative disposition of the acidic group on the proline ring and the zinc coordinating group is remarkably similar and is an important pharmacophoric feature. The dimensions of pharmacophoric features are measured in 3D and projected in 2D (Fig. 5). In this case, we derived the pharmacophore model using both HF and B3LYP DFT methods.

NEP inhibitors (see Fig. 6) also show the presence of an acidic group and a metal ion coordinating group. Hydrophobic groups are present at both ends. Despite differences in chemical structure, the positions of the acidic group and the zinc coordinating group are maintained in the same place. The hydrophobic region is less spread out than in ACE inhibitors. Important pharmacophoric features are collected in the form of the model presented in Fig. 6.

Figure 6 also illustrates conformational mapping of dual inhibitors. Mapping again emphasises the basic requirements of an acidic group, a zinc coordinating group and hydrophobic regions at both ends. An interesting feature is that the acidic group may be in either an ACE-like position or in an NEP-like position (cf. Figs. 5 and 6 for respective models). The derived non-skeletal pharmacophore model is shown.

Table 1 Correlation of calculated interaction energies with potency data

Drug	Experimental IC_{50} (nM)[a]	Active site model	Calculated interaction energy (kcal mol^{-1}) HF/6-31G
Trandolaprilat	0.93	ACE	−302.4
Perindoprilat	1.5– 3.5	ACE	−254.0
Ramiprilat	4.0	ACE	−214.0
Enalaprilat	4.50	ACE	−184.0
Lisinopril	4.70	ACE	−232.4
Quinaprilat	8.30	ACE	−505.2
BIR	1.20±0.2	NEP	−140.9
MDL100173	0.008	ACE	−505.2
MDL100173	0.11	NEP	−137.5
Designed drug		ACE	−324.5
		NEP	−100.6

[a] Taken from references 26, 28, 30–33

The overall pharmacophoric features can be summarised as follows:

- ACE/NEP inhibitors maintain an overall length of 12–13 Å but dual inhibitors are about 11 Å in length so as to be compatible with both active sites.
- An acidic group is required for binding/activity; however, its position varies according to active site requirements.
- In dual inhibitors, the acidic group is located either in an ACE-like position or in a NEP-like position and can probably be adjusted by slight rotation. The hydrophobic region at the ends is also small in dual inhibitors to maintain compatibility.
- Zinc coordinating carboxylate, phosphate or sulfhydryl groups are at roughly similar positions in all cases. Enzyme specificity is thus conferred not by the zinc coordinating group but rather by the position of other acidic groups.

Such minute differences between pharmacophore models can be highlighted only when accurate calculations have been performed prior to conformational mapping. Automated pharmacophore generation techniques can be applied to recognise pharmacophoric sites but not for detailed pharmacophore model generation.

ACE and NEP are synergistic in effect, therefore balanced dual inhibition is the ultimate design goal. To design balanced dual inhibitors, we must first understand the mechanism of action and the regulation of potency of both types of drug. To achieve this, we have made models for both ACE and NEP active sites. The pdb files employed to construct the ACE and NEP models were 1UZE [49] and 1R1H [50], respectively. The following residues in the two enzymes have been kept in ionized form:

ACE: K^+ 368, H^+ 383, E^- 384, H^+ 387, E^- 411, K^+ 511, H^+ 513, R^+ 522, H^+ 583
NEP: H^+ 583, E^- 584, H^+ 587, E^- 646, H^+ 711, R^+ 717

Both models are shown in Fig. 7. Both enzymes belong to the gluzincin family and contain the same HEXXH catalytic motif with a Zn^{2+} ion. The active site is highly positively charged in both cases.

Next, we ‘manually’ docked several drugs into the ACE/NEP model in order to understand how they interact with the catalytic motif and bring about the desired specificity. In this case, manual docking has certain advantages over automated docking due to the severe space constraints and highly charged active site. The active metabolite of the drug in the form of an ester was taken in cases where the acidic group was masked. The best interaction energies observed (each drug was docked several times until the best interaction was obtained) are listed in Table 1. It was noted that, although different possible conformations exist for

each drug (the example of enalaprilat is shown in suppl 1), only one or two actually fit within the constraints of the active site. The remaining conformers cannot bind (repulsion only is observed) and cannot even be docked. Enalaprilat conformations that could be docked are provided as ESM (see suppl 2, 3). Figure 8a depicts an ACE-specific drug docked in an ACE model, and Fig. 8b depicts a NEP-specific drug docked in an ACE model. Figure 8 clearly depicts how ACE-specific drugs fit in properly and interact favourably with the catalytic motif. On the other hand, the NEP-specific drug is conformationally not suited to fit into the ACE active site and can interact only just enough to bind to the metal ion of the ACE active site. This indicates the importance of minor differences in the

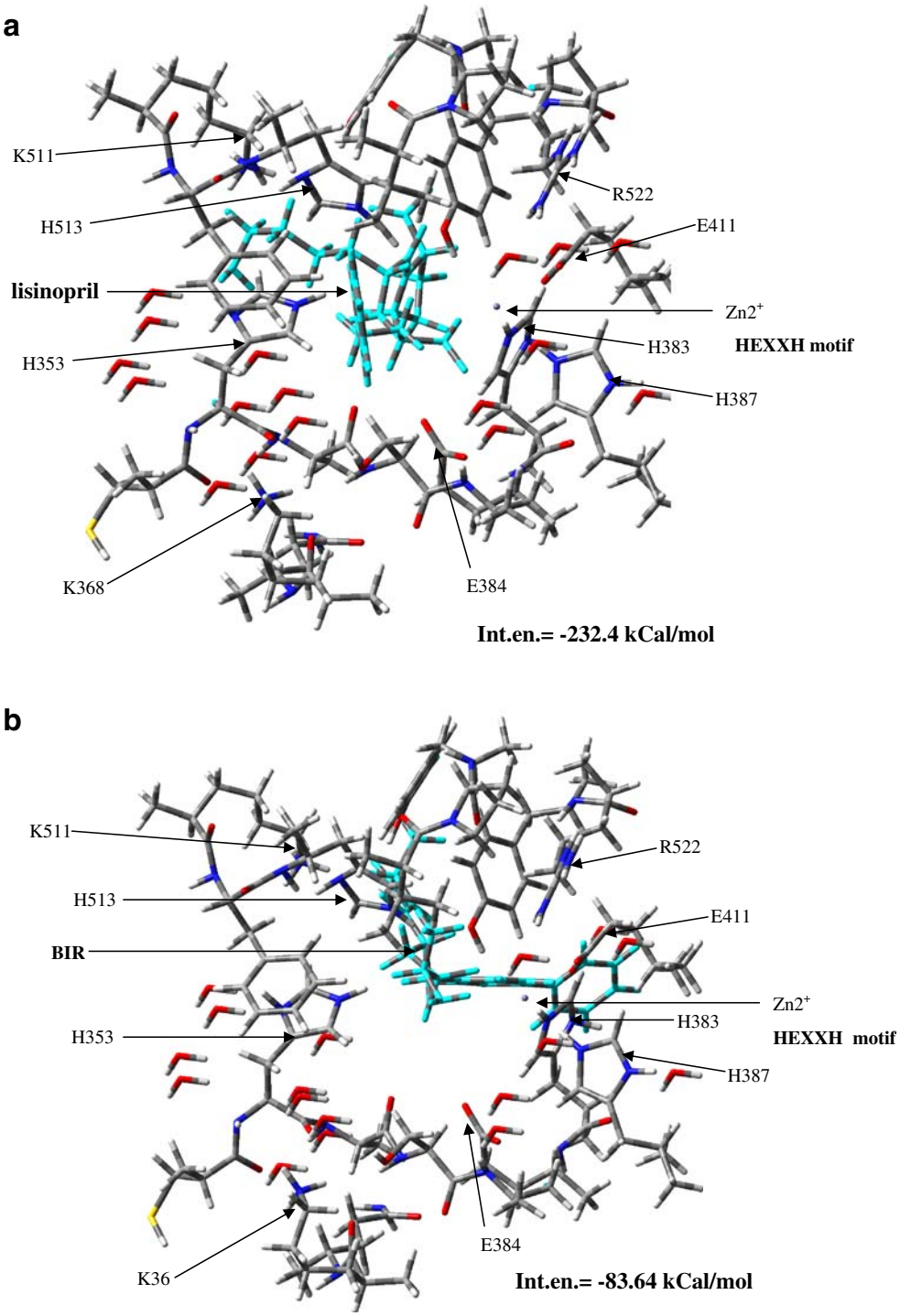

Fig. 8 **a** Lisinopril docked in ACE model. **b** BIR docked in ACE model

disposition of active site residues in the two enzymes, and the specificity thus conferred. Two main binding interactions have been identified: a metal binding group on the drug interacting with Zn^{2+}, and a metal binding group on the drug interacting with $H^{+}387$ mediated by a H-bonded water molecule. Figure 8a depicts the carboxylate group on lisinopril interacting with Zn^{2+} and $H^{+}387$. Zn^{2+} is held in the active site by $E^{-}411$. The remaining charged residues in

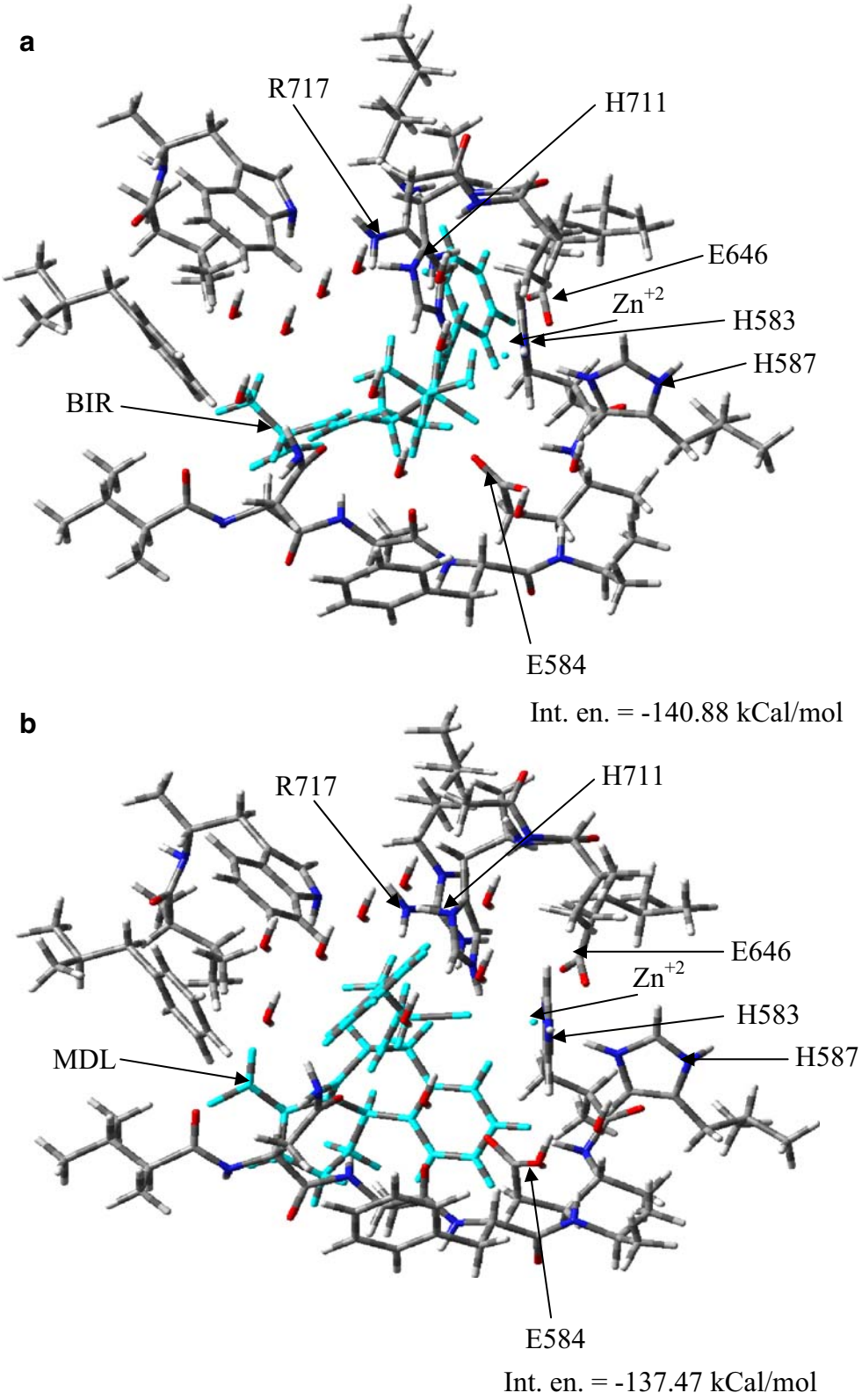

Fig. 9 **a** NEP-specific drug (BIR) in NEP model. **b** Dual inhibitor (MDL 100173) in NEP model

the ACE model collectively stabilize lisinopril. Figure 8b depicts BIR interacting with the ACE active site. Although it appears that this may not be the best orientation for BIR in the ACE model, in fact this is indeed the most favourable orientation as the zinc-binding group, phosphate in this case, is able to interact with Zn^{2+}; in any other orientation this alignment is disturbed. Also, in this case the water-mediated interaction with $H^{+}387$ has been disrupted. Docking of an ACE-specific drug in the ACE model is also presented in the form of a short video (see Suppl. 5).

Figure 9 illustrates the same NEP-specific drug (BIR) and a known dual inhibitor interacting with NEP active site residues. It also shows that NEP-specific drugs possess a size and conformation suited to that enzyme's active site and appropriate for optimal interactions with the catalytic motif. Figure 10 illustrates a known dual ACE/NEP inhibitor and a designed dual inhibitor interacting with the ACE active site. A designed dual inhibitor interacting with the NEP active site is shown in Fig. 11. It should be emphasised that all snapshots were captured keeping the catalytic motif in the same orientation to facilitate visual examination and comparison. The designed dual inhibitor shows considerable improvement over the existing dual inhibitor when judged in the light of balanced activity at both active sites. Designing

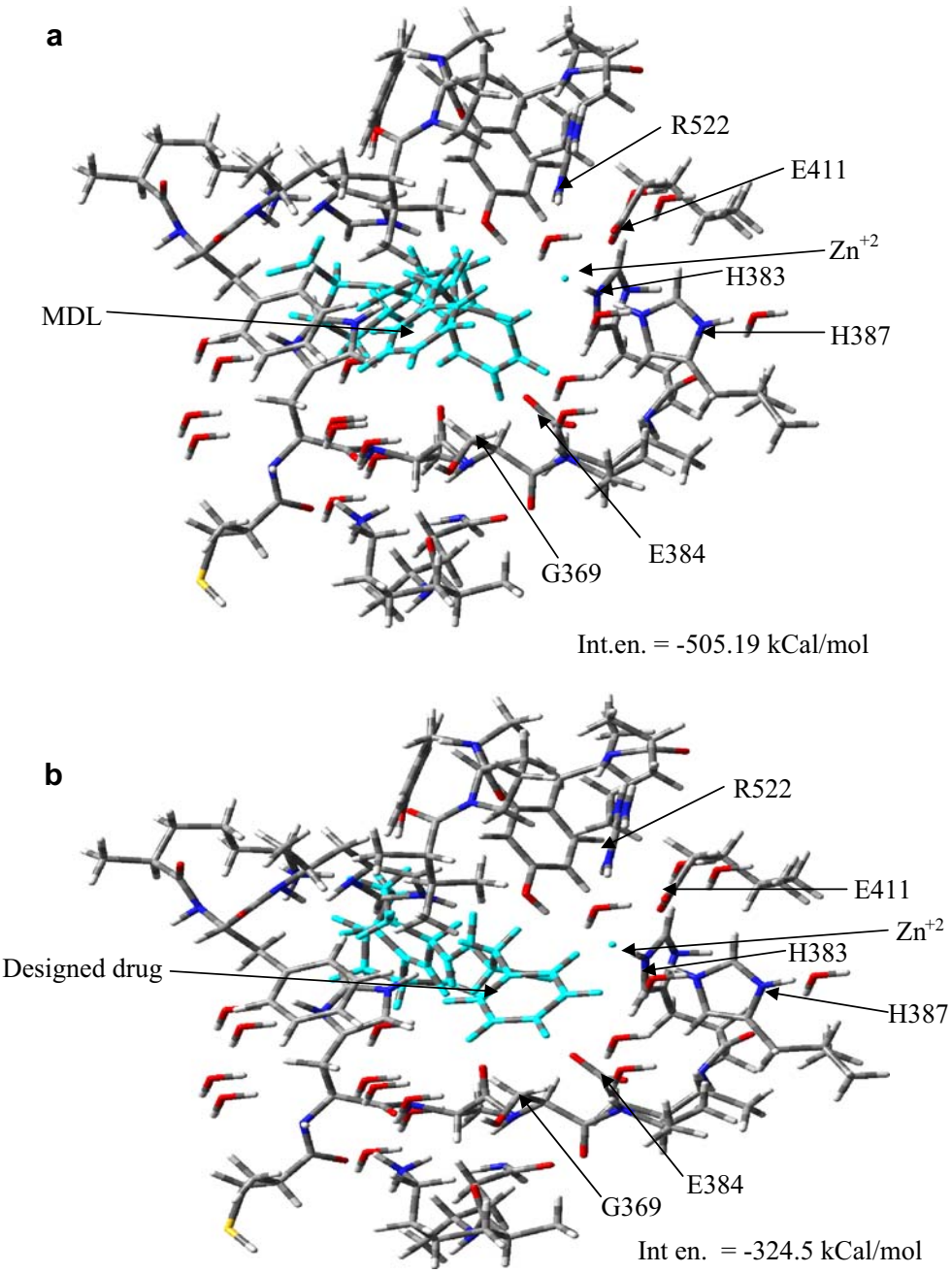

Fig. 10 **a** Dual inhibitor MDL 100173 in ACE model. **b** Designed drug in ACE model

was based entirely on derived pharmacophoric features, both conformational and electrostatic. The designed drug was also completely optimised before docking. Docking results are shown in Figs. 10 and 11 as mentioned above.

The calculated interaction energies for all drugs (Table 1) were in accordance with experimentally observed potency data, indicating that drug–receptor interactions are the key to understanding a drug's mechanism of action and potency. This correlation also indicates that this methodology can be applied successfully to predict the interaction of a designed drug with an enzyme active site, and hence an estimate of its activity as a dual inhibitor. Higher interaction energies (see Table 1) are suggestive of competitive inhibition as more potent drugs show more attractive interaction and can thus compete effectively with the natural substrate.

The designed drug interacted optimally at both enzyme active sites, indicating that it may be a better balanced dual inhibitor. "Balanced" multi-target designing is a difficult task due to differences in target enzymes. It is easy to design multi-target drugs without balanced activity but these are likely to lead to side effects. This stresses the need for accurate methodology.

It is encouraging to realise that ab initio methods can indeed be applied to such complicated design tasks, and can be driven towards actual correlation with activity data. This approach is 'unified and universal', as a single approach leads both to pharmacophore derivation and to understanding mechanistic aspects leading to drug design. In addition, this approach can be applied to the design of any type of inhibitor/antagonist.

Conclusions

This article describes the development and application of an accurate, cost-effective drug designing procedure that can be applied where careful design of 'balanced' dual inhibitors is needed. Pharmacophore models for ACE- and NEP-specific inhibitors have been derived. Drug–receptor interactions were studied in detail by making models of the ACE and NEP enzymes followed by docking of various inhibitors into these models. Accurate interaction energy calculations led to the design of balanced dual inhibitors.

Acknowledgments We gratefully acknowledge financial support by DST (Department of Science and Technology, New Delhi) project no.

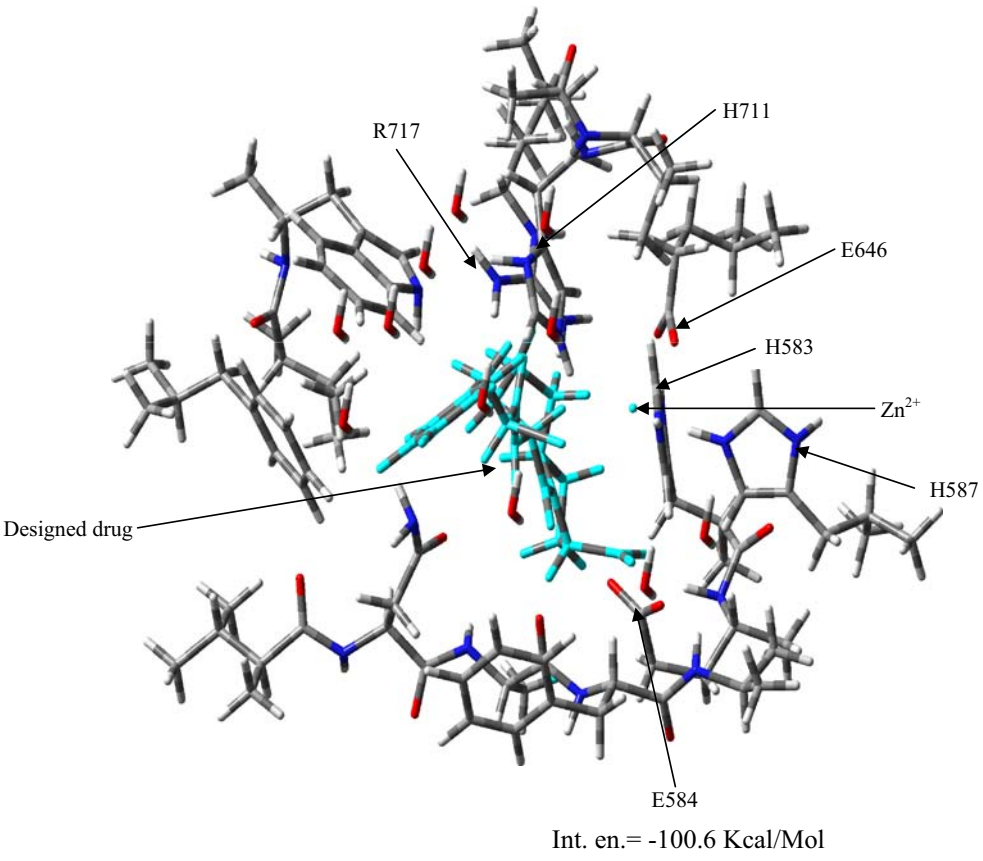

Fig. 11 Designed drug in NEP model

SR/S1/PC-06/2004. One of us (N. K. Rao) gratefully acknowledges DST for the Senior Research Fellowship.

References

1. Patrick G (ed) (2002) In: Medicinal Chemistry. BIOS Scientific, Oxford, pp 221–241
2. Cushman DW, Ondetti MA (1999) Nat Med 5:1110–1113
3. Ondetti MA (1994) Annu Rev Pharmacol Toxicol 34:1–16
4. Gupta SP (ed) (2006) QSAR and molecular modeling studies in heterocyclic drugs II. Springer, Berlin
5. Crippen GM (2008) Curr Comp Aided Drug Des 4:259–264
6. Zhou P, Tian F, Wu Y, Li Z, Shang Z (2008) Curr Comp Aided Drug Des 4:311–321
7. Meng EC, Shoichet BK, Kuntz ID (1992) J Comp Chem 13:505–524
8. Breda A, Basso LA, Santos DS, de Azevedo Jr WF (2008) Curr Comp Aided Drug Des 4:265–272
9. Dalton JA, Jackson RM (2007) Bioinformatics 23:1901–1908
10. Waszkowycz B, Perkins TDJ, Sykes RA, Li J (2001) IBM Syst J 40:360–378
11. Zhorov BS (1997) Arch Biochem Biophys 341:238–244
12. Yadav A, Singh SK (2005) THEOCHEM 723:205–209
13. Jain S, Yadav A (2008) Chem Biol Drug Des 71:271–277
14. Jandeleit-Dahm K (2006) J Hum Hypertens 20:478–481
15. Opie LH (1992) Angiotensin converting enzyme inhibitors. Wiley-Lisa, New York
16. Edwards C (1985) Lancet 325:30–34
17. Jackson B, Cubela RB, Conway EL, Johnston CI (1988) J Clin Pharmacol 25:719–724
18. Acharya KR, Sturrock ED, Riordan JF, Ehlers MRW (2003) Nat Rev Drug Disc 2:891–902
19. Molinaro G, Cugno M, Perez M, Lepage Y, Gervais N, Agostoni A, Adam A (2002) J Pharmacol Exp Ther 303:232–237
20. Johnston CI, Hodsman PG, Kohzuki M, Casley DJ, Fabris B, Phillips PA (1989) Am J Med 87:24S–28S
21. Wei L, Clauser E, Alhenc Gelas F, Corvol P (1992) J Biol Chem 267:13398–13405
22. Ehler MR, Riordan JF (1991) Biochemistry 30:7118–7126
23. Georgiadis D, Beau F, Czarny B, Cotton I, Yiotakis A, Dive V (2003) Circ Res 93:148–154
24. Dive V, Cotton J, Yiotakis A, Michaud A, Vassiliou S, Jiracek J, Vazeux G, Chauvet MT, Cuniasse P, Corvol P (1999) Proc Natl Acad Sci USA 96:4330–4335
25. Georgiadis D, Cuniasse P, Cotton J, Yiotakis A, Dive V (2004) Biochemistry 43:8048–8054
26. Laurent S, Boutouyrie P, Azizi M, Marie C, Gros C, Schwartz JC, Lecomte JM, Bralet J (2000) Hypertension 35:1148–1153
27. Weber M (1999) Am J Hypertens 12:139S–147S
28. Leung D, Abbenante G, Fairlie DP (2000) J Med Chem 43:305–341
29. Chevillard C, Jouquey S, Bree F, Mathieu M N, Stepniewski J P, Tillement JP, Hamon G, Corvol PJ (1994) Cardiovasc Pharmacol 4[suppl 23]:S1L–SL5
30. Oefner C, Roques BP, Fournie-Zaluski MC, Dale GE (2004) Acta Crystallogr D 60:392–396
31. Marie-Claire C, Ruffet E, Antonczak S, Beaumont A, Donohue MO, Fournie-Zaluski MC (1997) J Biochem 36:13938–13945
32. Barthelmebs M, Devissaquet M, Imbs JL (1989) Clin Exp Hypertens A11 [Suppl 2]:471–486
33. Sagnella GA (2002) J Renin Angiotensin Aldosterone Syst 3:90–95
34. Bralet J, Schwartz JC (2001) Trends Pharmacol Sci 22:106–109
35. Molineux G, Rouleau J, Adam A (2002) Curr Opin Pharmacol 2:131–141
36. Peng C, Ayala PY, Schlegel HB, Frisch MJ (1996) J Comput Chem 17:49–56
37. Peng C, Schlegel HB (1994) Israel J Chem 33:449
38. Petersson GA, Al-Laham MA (1991) J Chem Phys 94:6081–6090
39. Petersson GA, Bennett A, Tensfeldt TG, Al-Laham MA, Shirley WA, Mantzaris J (1988) J Chem Phys 89:2193–2218
40. Becke AD (1993) J Chem Phys 98:5648–5652
41. Breneman CM, Wiberg KB (1990) J Comput Chem 11:361–373
42. Schrodinger (2008) PHASE, Version 3.0. LLC, New York, NY
43. Dixon SL, Smondyrev AM, Rao SN (2006) Chem Biol Drug Des 67:370–372
44. Peitsch MC, Guex N (1997) Electrophoresis 18:2714–2723
45. Dennington R II, Keith T, Millam J, Eppinnett K, Hovell WL, Gilliland R (2003) GaussView, Version 3.09. Semichem, Shawnee Mission, KS
46. Frisch MJ, Trucks GW, Schlegel HB, Scuseria GE, Robb MA, Cheeseman JR, Montgomery JA Jr, Vreven T, Kudin KN, Burant JC, Millam JM, Iyengar SS, Tomasi J, Barone V, Mennucci B, Cossi M, Scalmani G, Rega N, Petersson GA, Nakatsuji H, Hada M, Ehara M, Toyota K, Fukuda R, Hasegawa J, Ishida M, Nakajima T, Honda Y, Kitao O, Nakai H, Klene M, Li X, Knox JE, Hratchian HP, Cross JB, Bakken V, Adamo C, Jaramillo J, Gomperts R, Stratmann RE, Yazyev O, Austin AJ, Cammi R, Pomelli C, Ochterski JW, Ayala PY, Morokuma K, Voth GA, Salvador P, Dannenberg JJ, Zakrzewski VG, Dapprich S, Daniels AD, Strain MC, Farkas O, Malick DK, Rabuck AD, Raghavachari K, Foresman JB, Ortiz JV, Cui Q, Baboul AG, Clifford S, Cioslowski J, Stefanov BB, Liu G, Liashenko A, Piskorz P, Komaromi I, Martin RL, Fox DJ, Keith T, Al-Laham MA, Peng CY, Nanayakkara A, Challacombe M, Gill PMW, Johnson B, Chen W, Wong MW, Gonzalez C, Pople JA (2004) Gaussian 03, Revision C.02. Gaussian, Wallingford CT
47. Hehre WJ, Ditchfield R, Pople JA (1972) J Chem Phys 56:2257–2261
48. Schlegel HB (1989) In: Bertran J (ed) New theoretical concepts for understanding organic reactions. Kluwer Academic, Dordrecht, pp 33–53
49. Natesh R, Schwager SLU, Evans HR, Sturrock ED, Acharya KR (2004) Biochemistry 43:8718–8724
50. Oefner C, Roques BP, Fournie-Zaluski MC, Dale GE (2004) Acta Crystallogr D 60:392–396